

# Expression/localization patterns of sirtuins (SIRT1, SIRT2, and SIRT7) during progression of cervical cancer and effects of sirtuin inhibitors on growth of cervical cancer cells

Sapna Singh · P. Uday Kumar · Suresh Thakur ·  
Shashi Kiran · Bijoya Sen · Shreya Sharma ·  
Vishnu Vardhan Rao · A. R. Poongothai ·  
Gayatri Ramakrishna

Received: 15 November 2014 / Accepted: 1 March 2015 / Published online: 21 March 2015  
© International Society of Oncology and BioMarkers (ISOBM) 2015

**Abstract** Sirtuins belong to the family of class III histone deacetylases; its role in neoplasia is controversial as both tumor-suppressive and promoting functions have been reported. There are very few reports available, where expressions of sirtuin isoforms are comprehensively analyzed during neoplasia. Therefore, in the present study, the expression of SIRT1, SIRT2, and SIRT7 during different stages of cervical cancer progression was analyzed. The normal cervical epithelium showed feeble expression of sirtuin isoforms, SIRT1, SIRT2, and SIRT7. A

significant increase in SIRT1 expression was noted in the cytoplasm as well as in the nucleus of proliferative layers of cervical epithelium in squamous intraepithelial lesions (SIL); however, in the squamous cell carcinomas (SCC), a heterogeneous pattern of SIRT1 expression varying from low to high was noted. A progressive increase in the expression of both SIRT2 and SIRT7 was noted during cancer progression in the following order: normal < preneoplasia < cancer. Cervical cancer cell lines, HeLa and SiHa, showed higher levels of SIRT1 and SIRT2 in comparison to the immortalized cell counterpart, HaCaT. Specific inhibitors of SIRT1 (Ex527) and SIRT2 (AGK2) impaired the growth of the cervical cancer cells, SiHa, but not of the HaCaT cells. SIRT1 inhibition caused cell death, while SIRT2 inhibition resulted in cell cycle arrest. In conclusion, we report the overexpression of SIRT2 and SIRT7 proteins in cervical cancer and suggest probable application of sirtuin inhibitors as therapeutic targets. Further, a specific increase in the levels of SIRT1 in intraepithelial lesion makes it a promising candidate for identification of preneoplastic changes.

**Electronic supplementary material** The online version of this article (doi:10.1007/s13277-015-3300-y) contains supplementary material, which is available to authorized users.

S. Singh · S. Kiran  
Centre for DNA Fingerprinting and Diagnostics, Hyderabad, India

S. Singh · P. U. Kumar · V. V. Rao  
National Institute of Nutrition, Hyderabad, India

S. Thakur · A. R. Poongothai  
BioGenex Lab Inc, Hyderabad, India

B. Sen · S. Sharma  
Laboratory of Cancer Cell Biology, Department of Research,  
Institute of Liver and Biliary Sciences (ILBS), D1 Block, Vasant  
Kunj, Delhi 110070, India

*Present Address:*  
G. Ramakrishna (✉)  
Laboratory of Cancer Cell Biology, Department of Research,  
Institute of Liver and Biliary Sciences (ILBS), D1 Block, Vasant  
Kunj, Delhi 110070, India  
e-mail: gayatrirama1@gmail.com  
e-mail: rgayatri@ilbs.in

**Keywords** Sirtuins · Cancer progression · Cervical cancer · AGK2 and EX527

## Abbreviations

SIRT Sirtuin  
IHC Immunohistochemistry  
SIL Squamous intraepithelial lesion  
SCC Squamous cell carcinoma

## Introduction

The Silent information regulator (SIR), sirtuins, belong to a highly conserved gene family from yeast to mammals and catalyze NAD<sup>+</sup>-dependent deacetylation or ribosylation of a variety of histone and non-histone proteins. The mammalian sirtuin family consists of seven members SIRT1–SIRT7, which are localized to different subcellular compartments. The various sirtuin isoforms modify a plethora of substrates involved in chromatin remodeling, cellular metabolism, DNA repair, and signaling events, thereby controlling diverse functions ranging from cellular proliferation to organismal aging. Sirtuins have been implicated in various pathologies such as aging, neurodegeneration, cardiovascular disorders, inflammation, immune dysfunction, and metabolic syndromes such as diabetes and obesity, etc. [1–3].

A connection between different sirtuin members and neoplasia has been suggested based on their roles in energy metabolism, chromatin remodeling, DNA damage response, and genomic stability. Interestingly, the tumor suppressors, p53 and Rb, are substrates of sirtuins. However, the role of sirtuins in neoplasia is controversial, as different sirtuin isoforms can have opposing functions of either tumor suppression or promotion depending on the cancer type [4, 5]. SIRT1 and SIRT3 can deacetylate p53 leading to its inactivation and thereby preventing growth arrest, senescence, or apoptosis and hence exercising oncogenic functions [6, 7]. On the contrary, the knockout mice models of SIRT1 and SIRT3 are prone to tumor development, thereby indicating their tumor-suppressive action [8, 9]. SIRT2 is mostly cytoplasmic in nature and considered a tumor suppressor, as it helps to regulate genomic integrity thereby controlling the cellular proliferation [10]. The tumor-suppressive role of mitochondrial SIRT4 is now linked to blocking of mitochondrial glutamine metabolism [11]. SIRT5 is localized to mitochondrial matrix and deacetylates the urea cycle enzyme carbamoyl phosphate synthetase 1 (CPS1); its link with cancer is still obscure. In the mouse model, SIRT6 acts as a tumor suppressor by inhibiting glycolytic metabolism [12]. The nucleolar form of SIRT7 can help maintain a transformed oncogenic state at least in the mouse fibroblasts [13].

The clinical relevance of sirtuin in human cancer has been assessed mostly on the basis of its expression pattern in tumors and the corresponding non-tumor samples. Using this approach, it has been shown that SIRT1 is upregulated in gastric cancers [14], colon cancer [15], and prostate cancer [16]. In hepatocellular cancer, both SIRT1 and SIRT7 are upregulated [17, 18]. SIRT2 expression is reduced in breast cancer, hepatocellular carcinoma, and gliomas compared to their normal counterparts supporting its tumor suppressive role [19]. Yet another report found high expression levels of SIRT2 and SIRT7 in node-positive breast cancer samples [20]. SIRT3 is deleted in most cancer types and most frequently in breast and

ovarian cancer [21]; its overexpression is noted in oral squamous cell carcinoma and cell lines [22]. SIRT6, when overexpressed, selectively killed cancerous cells [12], and it was frequently downregulated in hepatic cancer [23] thereby implicating a tumor-suppressive function.

Intriguingly, it has been noted that all sirtuin isoforms (SIRT1–7) in general are upregulated in squamous cell carcinoma of the skin [24]. On the contrary, a recent study has shown downregulation of all sirtuin isoforms (SIRT1–7) in head and neck squamous cell carcinomas [25]. Most cervical cancers are squamous in nature and originate at the squamous-columnar junction due to infection with human papilloma virus (HPV). The role of various sirtuin members in cervical cancer is still unexplored; however, it is important to note that HPV protein E7 when overexpressed in primary keratinocyte leads to higher expression level of SIRT1 [26]. In the present work, we evaluated the expression pattern of three sirtuin family members SIRT1, SIRT2, and SIRT7 during the progression of cervical carcinoma. These sirtuin members were chosen because of their distinct localization patterns at least in the cell lines; SIRT1 is nuclear, SIRT2 is cytoplasmic, and SIRT7 shows nucleolar localization [27]. Further, SIRT7 is the least studied of all the known sirtuin isoforms [28]. We now report significantly higher expression levels of SIRT1 and SIRT7 in intraepithelial lesions as compared to normal. Higher expression levels of SIRT2 were noted in the squamous cell carcinoma. The expression levels of SIRT1 and SIRT2 were higher in cervical cancer cell lines (SiHa and HeLa), and inhibition of SIRT1 and SIRT2 by their specific inhibitors [29], AGK2 and EX527, resulted in growth inhibition. Thus, the present work highlights the potential importance of sirtuins in progressive stages of cervical neoplasia.

## Materials and methods

### Tissue specimens

Approval was obtained from the institutional research ethics board. Archived tissue materials were retrospectively reviewed in a total of 140 cases: normal cervix/chronic cervicitis ( $N=41$ ), squamous intraepithelial lesions (SIL) ( $N=32$ , includes both low (LSIL) and high (HSIL) grade lesions), and invasive cervical squamous cell carcinoma (SCC) ( $N=67$ ). The patients were in the age group ranging from 25 to 70 years (Table 1). Average ages for the different histopathological groups were similar.

### Immunohistochemistry

Paraffin tissue sections (3  $\mu\text{m}$ ) were placed on poly-L-lysine-coated slides and were deparaffinized in xylene followed by successive rehydration in alcohol changes.

**Table 1** Histopathological distribution of clinical samples used in the study

Diagnosis	Histopathology	Mean age	Number of cases (%)
Normal cervix	Inflammatory, benign non-neoplastic	47.03±13.35(25–70)	41 (29)
Squamous intraepithelial lesion (SIL)	LSIL (14), HSIL (18)	46.2±8.36(30–63)	32 (23)
Squamous cell carcinoma (SCC)	SCC grade 1(9), SCC grade 2(23), SCC grade 3(35)	44.38±9.33(27–60)	67 (48)
Total			140

Antigen retrieval was carried out, using Citra Plus Ready-to-Use Antigen Retrieval Solution (BioGenex Antigen Retrieval systems, USA) by microwave heat-induced epitope retrieval. Peroxide and power blocking were performed using a BioGenex kit according to manufacturer's instructions. Serial sections were then incubated with various antibodies viz SIRT1, SIRT2, SIRT7, p27, and Ki67 (Supplementary Data 1), followed by treatment with Super Enhancer (BioGenex, Fremont, CA, USA) for 20 min. The sections were then incubated with polymer-horseradish peroxidase secondary antibody, and final color development was done by treatment with diaminobenzidine (DAB) as a chromogen. Sections were counterstained with hematoxylin, dehydrated, cleared with xylene, and mounted in D.P.X. mountant (Himedia, India). The final brown color after reaction product was evaluated by light microscopy. The following positive controls were used for various antibodies: Ki67, tonsil; SIRT1 and SIRT2, colon cancer; SIRT7, breast cancer; and p27, skin biopsy. For negative control, a serial section was processed without primary antibody incubation step; however, the section was incubated with the secondary antibody. Positive and negative controls were also used to test the background error.

#### Evaluation of immunohistochemistry (IHC)

Immunoreactivity was considered significant when the immunostaining with DAB was observed in more than 10 % cells of the tissue. A semiquantitative scoring system was adopted by scoring the staining intensity together with the extent of the area stained as described earlier [30]. IHC-stained slides were scored as negative (0), low (1–2), and strong (2–3). Stained slides were evaluated by a single pathologist using light microscope (Nikon Eclipse E800), and no image analysis software was used for evaluation. Coexpression of different sirtuin members and p27/Ki67 was carried similar to the study on differential expression of proteins in cervical cancer as described previously by Lomnyska et al. [31].

#### Cell culture, inhibitor treatment, and viability assay

The human cervix epithelium carcinoma cell lines HeLa and SiHa and immortalized non-transformed keratinocyte cell line HaCaT (obtained from NCCS, Pune, India) were maintained in DMEM medium (HyClone Thermo Scientific) supplemented with 10 % fetal bovine serum, glutamine, and antibiotics (penicillin/streptomycin). Cells were maintained at standard cell culture conditions (37 °C, 5 % CO<sub>2</sub> in a humidified incubator) as recommended. For treatment with sirtuin inhibitors, the cells were plated at a density of  $3 \times 10^3$  cells per well in a 24-well tissue culture dish. The cells were treated with either inhibitors, Ex527 (Tocris bioscience, Cat. No. 2780), AGK2 (Sigma, Cat. No. A8231), or vehicle (DMSO) for 24 h followed by change to fresh medium and cultured for an additional 7 days. To check the growth, the cells were fixed with 2 % paraformaldehyde for 30 min at room temperature, stained with 0.5 % crystal violet, and the dye was solubilized with 1 % SDS, and the absorbance was read at 540 nm on a spectrophotometer [32].

#### Immunoblot analysis

Immunoblot assay was performed as described earlier [33]. Briefly, the cellular homogenate was prepared from the three cell lines, HaCaT, HeLa, and SiHa and proteins separated on SDS-polyacrylamide gel, transferred to polyvinylidene difluoride membranes, and incubated with the various sirtuin primary antibodies. Detection was done using the ECL Prime reagent (GE Healthcare, Little Chalfont, UK) according to manufacturer's instructions. Replicate experiments were done, and immunoblot was quantified by densitometry (ImageJ 1.17 software; National Institutes of Health (NIH), Bethesda, MD; available by ftp at [zippy.nimh.nih.gov/or](http://zippy.nimh.nih.gov/or) at <http://rsb.info.nih.gov/nih-image>; developed by Wayne Rasband, National Institutes of Health, Bethesda, MD). The sirtuin expression was normalized to tubulin, which served as the loading control, and relative fold change was calculated as follows: (a) for cervical cancer cells (HeLa and SiHa) relative to the immortalized cell line, HaCaT, and (b) for the experimental group with inhibitor treatment relative to the untreated control cells.

## Immunofluorescence

For studying the localization of various sirtuin isoforms, cells were plated and grown on chambered slides until a confluence of 70 % was reached. The cells were fixed in 3 % formaldehyde for 5 min and then treated with 0.1 % Triton-X, blocked with 2 % bovine albumin serum (BSA) for 30 min. Following blocking, anti-SIRT1, SIRT2, or SIRT7 antibodies (Abcam) at a dilution of 1:100 were added and allowed to incubate for overnight at 4 °C. Primary antibody was removed by washing with PBS, followed by incubation with Alexa Fluor 488 goat anti-rabbit secondary antibody (Invitrogen, USA) for 1 h at 37 °C in the dark and mounted in VECTASHIELD Mounting Media containing 4, 6-diamidino-2-phenylindole (DAPI) (Molecular Probes) and anti-fade. Images were captured on an inverted epifluorescence microscope (Olympus 1X51, Tokyo, Japan).

## Total RNA isolation and cDNA synthesis

Total RNA was isolated from the three cell lines viz HaCaT, HeLa, and SiHa using the TRIzol Reagent (Life Technologies, USA). RNA was dissolved in nuclease-free water and subjected to DNase treatment using DNA-Free RNA™ Kit (Zymo Research Inc., Orange, CA) following manufacturer's instructions. The quality and quantity of extracted RNA were tested by spectrophotometrical method by checking the absorption in wavelengths of 260 and 280 nm, followed by calculating the ratio of 260/280 nm. The RNA integrity was also checked by evaluating the 18S and 28S rRNA signals by running 1 µl of total RNA on denaturing agarose gel stained with ethidium bromide.

For making the complementary DNA (cDNA), 1 µg of RNA was reverse transcribed using SuperScript III Reverse Transcriptase (Life Technology, USA) in 20 µl reaction volume containing 2.5 mM MgCl<sub>2</sub>, 2 mM deoxyribonucleoside triphosphates, 0.5 µg of random hexanucleotide primers, and 1 U of RNaseOUT. The mixture was then incubated at 50 °C for 60 min, and reaction was stopped by incubating the mixture at 70 °C for 15 min. The cDNA thus prepared was then used as a template for further real-time polymerase chain reaction (PCR).

## Quantitative real-time PCR

cDNA was synthesized as described above, and quantitative reverse transcriptase polymerase chain reaction (qRT-PCR) was performed using Power SYBR Green PCR Master Mix (Applied Biosystems) and an Applied Biosystems 7300 Real-Time PCR System. The gene expression level was normalized against GAPDH messenger RNA (mRNA) which served as an internal control. The primers used were as follows: *SIRT1* primers with

forward (5'-ACGCTGGAACAGGTTGCGGG-3') and reverse (5'-AGCGGTTTCATCAGCTGGGCAC-3') and a product size of 167 bp; *SIRT2* primers with forward (5'-TCACACTGCGTCAGCGCCAG-3') and reverse (5'-GGGCTGCACCTGCAAGGACG-3') with a product size of 228 bp; *SIRT7* primers with forward (5'-ACCTGCCAAATATGATGAC-3') and reverse (5'-TCATACCAGGAAATGAGCTT-3') with a product size of 236 bp. Dissociations curves were generated to ensure that only one product was amplified. The relative gene expression was calculated using ( $-\Delta\Delta C_t$ ) method as described earlier [34]. The relative gene expression values were subsequently expressed as fold change by using the  $2^{-\Delta\Delta C_t}$  method. Fold change in sirtuin mRNA expression in cancerous cell lines HeLa and SiHa was calculated relative to the counterpart immortalized cell line, HaCaT.

## Cell cycle analysis

Cells were fixed at different time points with a mixture of 70 % ethanol and methanol mix (1:1) for 24 h, followed by treatment with RNase A (5 µg/ml) and staining with 50 µM propidium iodide (PI). The cells were then subjected to flow cytometry (BD Biosciences FACSAria III).

## Statistical analysis

Statistical analysis for immunohistochemical expressions was performed by  $\chi^2$  test using the software, PEPI version 4.0 (by Abramson and Gahlinger). All in vitro experiments were done in triplicate and results expressed as Mean±SEM. Data comparison within multiple groups was done using one-way ANOVA analysis (MS—Excel). Post hoc comparison of the means was carried out using Tukey's multiple comparison tests. *P* value ≤0.05 was considered statistically significant.

## Results

### Histopathological data

The chronology of events leading to cervical cancer involves chronic cervicitis progressing to squamous cell intraepithelial lesions (SIL) which finally culminate as invasive squamous cell carcinoma (SCC). The present study included a total of 140 cervical biopsy samples which were classified as non-neoplastic, preneoplastic lesions, and squamous cell carcinoma. The clinicopathological features of the specimens are described in Table 1. A total of three normal cervical epithelia that were without any abnormal cervical pathology were grouped together with cases of cervicitis (*N*=38) as non-neoplastic grade. A total of 32 samples belonging to low-grade (LSIL) and high-grade (HSIL) squamous cell intraepithelial lesions were grouped together as preneoplastic

squamous intraepithelial lesion (SIL). The neoplastic group comprised of a total of 67 cases of squamous cell carcinomas (SCC, N=67).

#### Expression and localization pattern of sirtuins in different grades of cervical lesions

The expression of sirtuin family members SIRT1, SIRT2, and SIRT7 in the non-neoplastic, preneoplastic, and neoplastic lesions of the cervix was analyzed by immunohistochemistry (IHC). The expression of SIRT1 was almost negligible in majority of the non-neoplastic cervical epithelium, while higher expression was noted in preneoplastic intraepithelial lesions, SIL (Fig. 1a and Supplementary Data 2). A significant

increase in SIRT1 expression was noted in both the cytoplasm and nucleus of basal, parabasal, intermediate, and superficial layers of cervical epithelium in the preneoplastic lesions compared to the non-neoplastic group (Table 2, Supplementary Data 3). There was no apparent difference in SIRT1 expression among the two grades of SIL, i.e., LSIL and HSIL (data not shown). Intriguingly, in squamous cell carcinoma, a heterogeneous staining pattern for SIRT1 was noted ranging from no expression to high levels of cytoplasmic or nuclear expression (Supplementary Data 2).

The expression of SIRT2 was mostly absent in the entire epithelium of normal cervix and also the preneoplastic squamous cell intraepithelial lesions in majority of the samples. Less than 25 % of the total samples in normal and SIL showed

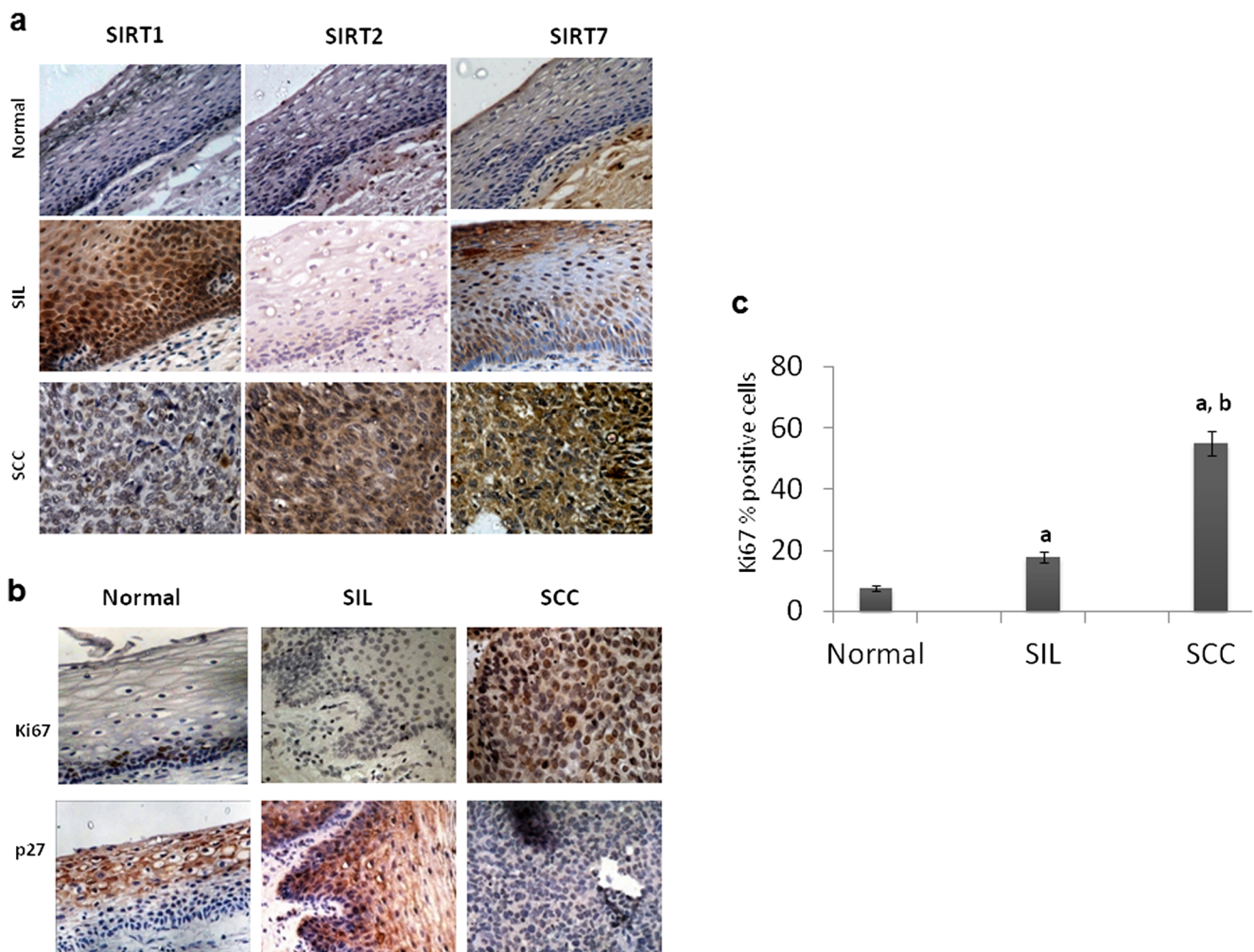


**Fig. 1** **a** Representative images of immunohistochemical staining patterns of sirtuin members, SIRT1, SIRT2, and SIRT7 in the normal cervix, intraepithelial lesion (SIL), and squamous cell carcinoma (SCC). Conventional immunohistochemistry was performed using DAB as a chromogen. Note a weak staining for all the three sirtuin members in the normal non-neoplastic cervical tissue (40X). An intense nuclear and cytoplasmic staining of SIRT1 is observed in all the layers in the benign intraepithelial lesion (40X). Note a progressive increase in expression of SIRT2 and SIRT7 from benign to squamous cell carcinoma (SCC; 40X). **b** Expression of proliferative marker Ki67 and growth arrest marker p27

during the cervical cancer progression. Representative images of various stages of cervical cancer progression showing immunostaining pattern for Ki67 and p27. Note a strong staining pattern for Ki67 in squamous cell carcinoma (SCC) with an almost absence of p27 indicative of an inverse association. **c** A bar diagram showing a significant increase in the percentage of Ki67-positive cells in intraepithelial lesion and the squamous cell carcinoma compared to the non-neoplasia. Letters *a* and *b* indicate significant difference with control and squamous cell intraepithelial lesion, respectively ( $P < 0.05$ )

**Table 2** Immunohistochemical expression profile of SIRT1, SIRT2, and SIRT7 in normal, preneoplastic squamous intraepithelial lesion (SIL) and squamous cell carcinoma (SCC)

Variables	Cytoplasm				Nuclear			
	Negative	Low	High	<i>P</i> value	Negative	Low	High	<i>P</i> value
<b>SIRT1</b>								
Normal ( <i>N</i> =41)	29(70 %)	6(15 %)	6(15 %)		30(73 %)	5(12 %)	6(15 %)	
cSIL ( <i>N</i> =32)	14(44 %)	5(15 %)	13(41 %)	0.032 <sup>a*</sup>	13(41 %)	0(0 %)	19(59 %)	0.001 <sup>a*</sup>
SCC ( <i>N</i> =67)	34(51 %)	10(15 %)	23(34 %)	0.067 <sup>b</sup> , 0.794 <sup>c</sup>	45(67 %)	2(3 %)	20(30 %)	0.052 <sup>b*</sup> , 0.015 <sup>c*</sup>
<b>SIRT2</b>								
Normal ( <i>N</i> =42)	31(74 %)	8(19 %)	3(7 %)		27(64 %)	5(12 %)	10(24 %)	
SIL ( <i>N</i> =32)	21(66 %)	3(9 %)	8(25 %)	0.074 <sup>a</sup>	25(78 %)	0(0 %)	7(22 %)	0.115 <sup>a</sup>
SCC ( <i>N</i> =67)	20(30 %)	30(45 %)	17(25 %)	0.000 <sup>b*</sup> , 0.001 <sup>c</sup>	54(81 %)	5(7 %)	8(12 %)	0.159 <sup>b</sup> , 0.148 <sup>c</sup>
<b>SIRT7</b>								
Normal ( <i>N</i> =34)	19(56 %)	13(38 %)	2(6 %)		26(76 %)	3(9 %)	5(15 %)	
SIL ( <i>N</i> =26)	11(42 %)	5(19 %)	10(39 %)	0.006 <sup>a*</sup>	19(73 %)	0(0 %)	7(27 %)	0.104 <sup>a</sup>
SCC ( <i>N</i> =62)	9(15 %)	18(29 %)	35(56 %)	0.000 <sup>b*</sup> , 0.023 <sup>c*</sup>	55(89 %)	1(1 %)	6(10 %)	0.177 <sup>b</sup> , 0.102 <sup>c</sup>

<sup>a</sup> *P* value differences between Normal and SIL

<sup>b</sup> *P* value differences between Normal and SCC

<sup>c</sup> *P* value differences between SIL and SCC

\**P*<0.05

scanty to feeble staining for SIRT2 which was restricted to basal and parabasal layer. In contrast, an increase in cytoplasmic expression of SIRT2 was noted in majority (approx 89 %) of squamous cell carcinoma specimens (Fig. 1a, Table 2, and Supplementary Data 3). The SIRT2 immunoreactivity was noted in the entire tumor region.

Similar to the other two sirtuins described above, the expression of SIRT7 was feeble in the normal cervical epithelium. However, a progressive increase in SIRT7 expression was noted in the cytoplasm of preneoplastic and carcinoma cases as compared to the normal cervix (Fig. 1a, Table 2, and Supplementary Data 3), whereas nuclear expression appeared reduced somewhat. In the SIL cases, the entire abnormal cervical epithelium scored positive for SIRT7 expression.

Association of proliferative marker Ki67 and growth arrest marker p27 with sirtuin expression together with their topological distribution in the cervical epithelium

The foregoing analysis indicated a differential expression pattern of sirtuin isoforms during the sequence of events leading to squamous cell carcinoma. SIRT1 expression was significantly higher in preneoplasia, while higher SIRT2 and SIRT7 expression correlated with squamous cell carcinoma. In view of this, we asked how this altered expression pattern of sirtuin isoforms might correlate with the proliferative index. Hence, the expressions of cell proliferation marker Ki67, and growth arrest marker p27, a cyclin-dependent kinase inhibitor (CDKI), were measured. Usually, an inverse association exists

between expression levels of p27 and Ki67 between normal and cancer samples, and present results showed a similar pattern (Fig. 1b). As expected, the Ki67 labeling index was maximum in squamous cell carcinoma (Fig. 1b), and the p27 levels were comparatively high in the SIL cases compared to SCC (Fig. 1c and Supplementary Data 3).

The Ki67 labeling index, p27 expression pattern, and its topological distribution in relation to sirtuins were as follows: (a) *non-neoplastic cases*: Majority of the samples (80 %, 33/41) showed p27 positivity in the suprabasal and superficial layers while the basal layer was totally devoid of it; on the other hand, Ki67 expression was almost absent except for one or two cells only in the parabasal epithelium (Ki67 labeling index, 2/100); expression of SIRT 1,2, and 7 showed either negative or very feeble expression which was limited to only basal and parabasal regions; (b) *squamous intraepithelial lesions*: The entire epithelium consisting of basal, parabasal, intermediate, and superficial layers showed intense p27 staining, and this pattern was also seen for SIRT1 expression as described above. A significant positive association was observed for SIRT1 and p27 in the intraepithelial lesions (Table 3 and Supplementary Data 3). The Ki67 expression was noted only in the parabasal layer of the cervix epithelium (Ki67 labeling index, 30/100). The expression of SIRT2 (only in a few cases) and SIRT7 was limited to basal or suprabasal regions; (c) *squamous cell carcinoma*: The p27 expression was either feeble (70 %, 46/67) or negative in tumors (30 %, 21/67); in contrast, prominent Ki67 expression was noted in majority of the tumors (60 %, 60/100). To summarize, we found an

**Table 3** Co-expression of sirtuin isoforms and p27 in normal, squamous intraepithelial lesion (SIL), and squamous cell carcinoma (SCC)

Histopathology	Sirtuins	p27		P value
		+	-	
Normal/ASCUS	SIRT1(N=41)	+	15(37 %)	0.067
		-	2(5 %)	
	SIRT2(N=37)	+	12(33 %)	0.214
		-	6(16 %)	
	SIRT7(N=27)	+	13(48 %)	0.711
		-	4(15 %)	
SIL	SIRT1(N=32)	+	19(59 %)	0.031*
		-	4(12 %)	
	SIRT2(N=29)	+	9(31 %)	0.730
		-	4(14 %)	
	SIRT7(N=24)	+	11(46 %)	0.070
		-	7(29 %)	
SCC	SIRT1(N=67)	+	30(45 %)	0.793
		-	13(19 %)	
	SIRT2(N=65)	+	35(54 %)	0.522
		-	13(20 %)	
	SIRT7(N=60)	+	37(61 %)	0.558
		-	18(30 %)	

\* $P < 0.05$ 

apparent inverse association between the Ki67 and p27 expression levels in cervical cancer stages, and significant positive correlation between SIRT1 and p27 expression in intraepithelial lesions, that was not observed with SIRT2 or SIRT7.

#### Expression and localization pattern of sirtuins in cervical cancer cell lines

As the above work suggested a role for different sirtuin isoforms in preneoplastic and cancerous lesions in cervical cancer, we next evaluated if their expression levels are also altered in cervical cancer cell lines and whether sirtuin inhibitors might have any effect on growth of these cell lines. The expression levels and localization patterns of SIRT1, SIRT2, and SIRT7 were therefore checked in a panel of commonly used cervical cancer cell lines, HeLa and SiHa, and the immortalized non-transformed keratinocyte counterpart cell line, HaCaT. The real-time PCR analysis showed a significant fivefold increase in SIRT1 levels in SiHa cell and almost a twofold higher level in HeLa cells when compared to the mRNA expression in the immortalized, HaCaT cells (Fig. 2a). However, no significant change in expression levels of SIRT2 and SIRT7 mRNA was observed. Next, the protein levels of sirtuin members in the three different cell lines were analyzed by immunoblot assay using specific antibodies (Fig. 2b and Supplementary Data 4). The experiments were done in replicates and fold change in sirtuin levels in HeLa and SiHa cells

was compared to HaCaT (Fig. 2c). Almost fivefold increase in SIRT1 protein level was noted in cancerous cells, HeLa and SiHa cells when compared to the immortalized counterpart HaCaT cells. For both SIRT2 and SIRT7 proteins, we noted two distinct signals, with differing electrophoretic mobility, in immunoblot, and this has been reported by other workers as well [33, 35]. Contrary to mRNA expression, both HeLa and SiHa cells showed significantly higher levels of SIRT2 protein levels, at least for the 44.7 kDa isoform, compared to HaCaT cells. SIRT7 protein levels were almost comparable in all the three cell lines. Next, the localization pattern of all the three sirtuin members was evaluated in HaCaT and SiHa cells. Immunofluorescence studies revealed SIRT1 to be predominantly localized in the nucleus; a prominent cytoplasmic staining was noted for SIRT2, whereas SIRT7 showed nucleolar localization. No apparent difference in localization pattern of sirtuins was noted between the cancerous cell, SiHa, and the immortalized cell, HaCaT (Fig. 2d).

#### Specific inhibitors of sirtuins inhibit growth of cervical cells

To test if increased levels of sirtuin isoforms in cervical cancer cells have a function in cellular proliferation, SiHa cells were treated with Sirtinol which in general inhibits all the sirtuin isoforms. It was noted that high doses of Sirtinol (starting from 50  $\mu\text{M}$  onwards) were growth inhibitory (Supplementary Data 5). Cell stained with propidium iodide (PI) and subjected to flow cytometric analysis showed prominence of sub G0 cells indicative of cell death when treated with 100  $\mu\text{M}$  of Sirtinol. Next, it was evaluated if inhibiting the different sirtuin members using specific inhibitors will have any differential affect on growth of SiHa and HaCaT cells. For this, the cells were treated with Ex527 and AGK2 which specifically inhibit SIRT1 and SIRT2, respectively, and growth was monitored by the crystal violet assay method. A dose-response curve of AGK2 and Ex527 indicated that a dose above 30  $\mu\text{M}$  is growth inhibitory to cancerous cells but not the immortalized HaCaT cells (data not shown). We therefore did a comparative growth analysis of SiHa, HeLa, and HaCaT by treating the cells with a 40  $\mu\text{M}$  dose of each of the inhibitors for 24 h followed by release in fresh medium (Fig. 3a). The immortalized HaCaT cells showed an initial growth inhibition followed by a good recovery when the inhibitors were removed. However, a significant reduction in cell viability of both SiHa and HeLa cells was observed even after the removal of the sirtuin inhibitors (Fig. 3a). Interestingly, it was noted that growth inhibition in cancer cell lines by Ex527 (specific inhibitor of SIRT1) was also accompanied by changes in cellular morphology of HeLa and SiHa cells, which appeared more slender and elongated (Fig. 3b). Propidium iodide staining was performed to evaluate whether growth inhibition by Ex527 and AGK2 is due to cell death or cell cycle arrest. Cell cycle distribution

analysis showed that both SIRT1 and SIRT2 inhibitors caused only subtle changes in the cell cycle distribution pattern of immortalized HaCaT cells (Fig. 3c). In contrast, SiHa cells treated with SIRT2 inhibitor AGK2 showed a prominent sub G0 phase indicative of massive cell death, while cells treated with SIRT1 inhibitor Ex527 resulted in growth arrest in G1/G0 phase of cell cycle. Next, we analyzed the expression of SIRT1 and SIRT2 proteins in cells treated with sirtuin inhibitors, EX527 and AGK2, by immunoblotting. Intriguingly, the SIRT1 inhibitor AGK2 showed a decrease in protein levels of both SIRT1 and SIRT2 in the cervical cancer cell line HeLa at 24 and 48 h following treatment (Fig. 3d). On the other hand, the SIRT1 inhibitor Ex527 showed no significant change in expression pattern of SIRT1 or SIRT2 proteins as seen by immunoblot.

## Discussion

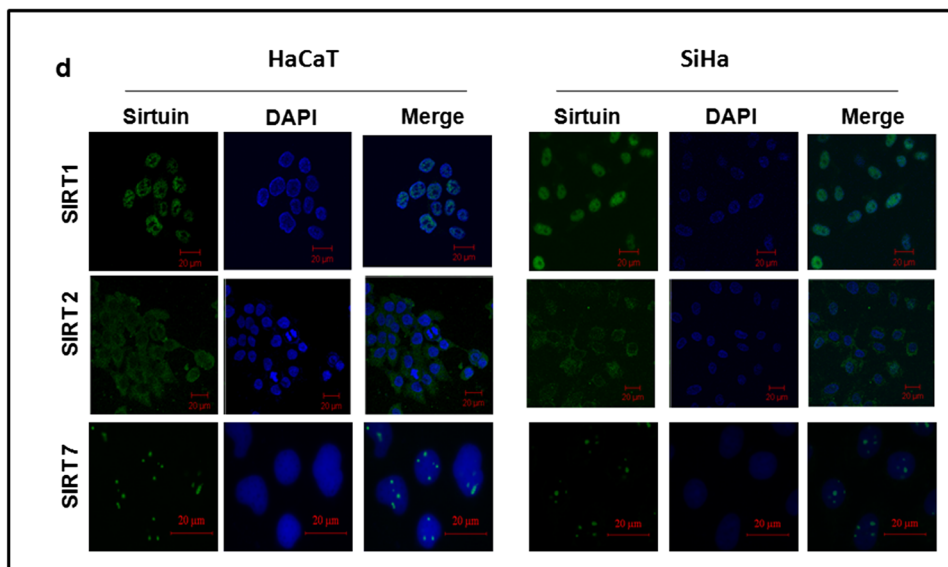
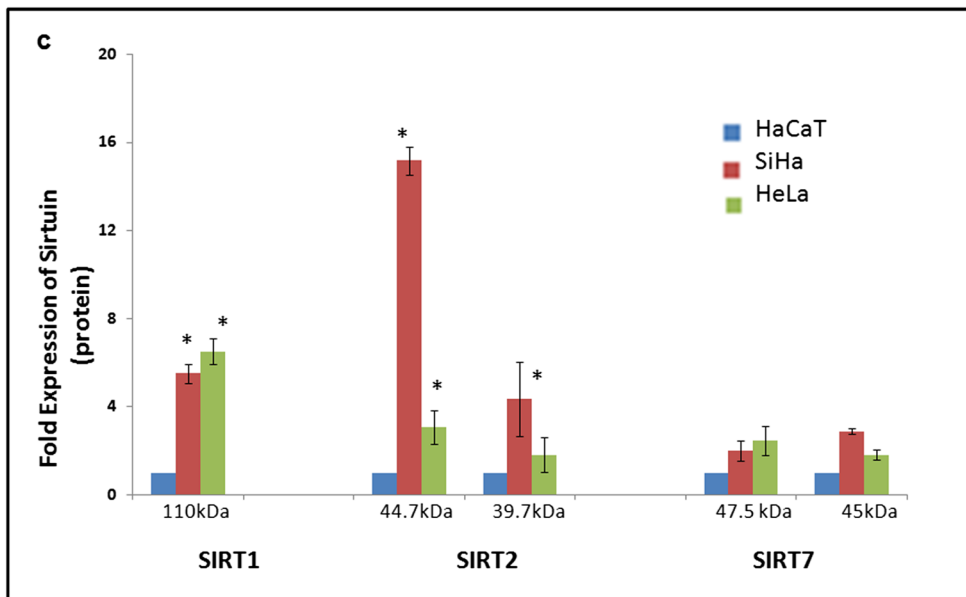
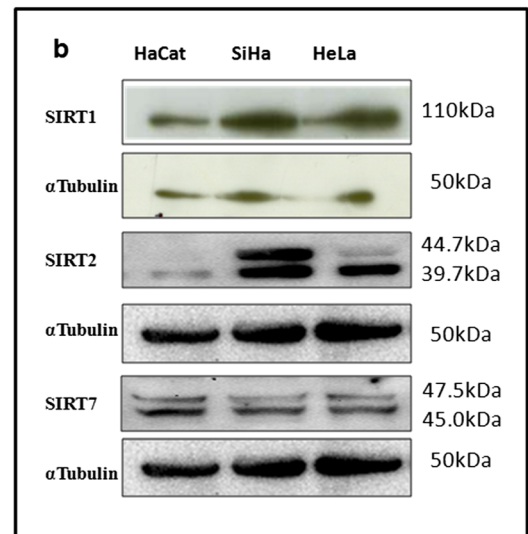
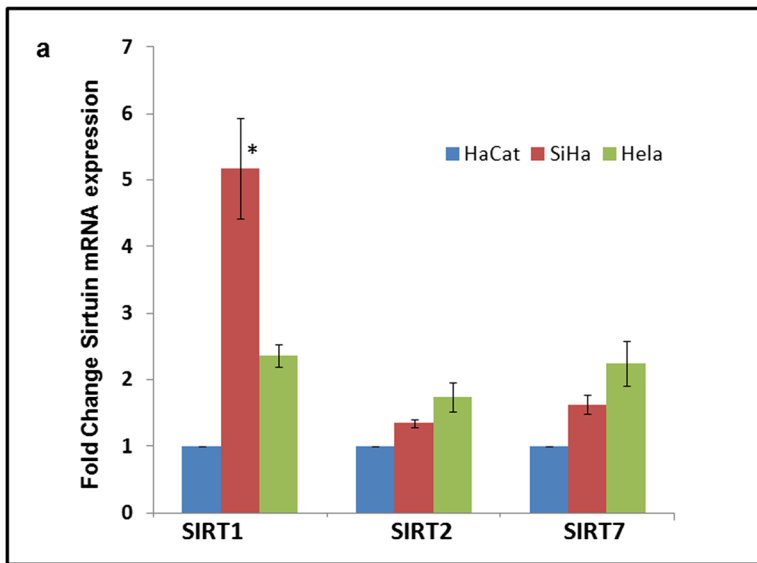
Cervical cancer is the second most common cancer affecting women worldwide and the most prevalent cancer among women in rural India [36]. Besides infection with HPV, other host factors like genetic and immunological aspects play an important role in the progression towards cervical neoplasia [37]. A multitude of target proteins involved in cellular growth and metabolism are affected by deacetylation/ribosylation activities of sirtuins, thereby making it a strong candidate influencing neoplastic transformation. However, the role of sirtuin isoforms appear complex, with reports describing their role in both tumor suppression and progression. There is limited information regarding the roles of sirtuins in cervical cancer. However, reports using cell lines have indicated sirtuin inhibition in SiHa cells leads to growth arrest [38], and a causal link between HPV-E7 oncogenic proteins leading to increased levels of SIRT1 has been described [26]. Since there are no available data on the sirtuin expression and distribution in cervical mucosa, we analyzed the same during progression from the well-defined precursor lesion, squamous intraepithelial lesion (SIL) to squamous cell carcinoma (SCC). Additionally, we tried correlating the expression of sirtuins with both the proliferation marker (Ki67) and the growth arrest marker (p27). Our data revealed that SIRT1 expression is more prominent only in preneoplasia, while a progressive increase in SIRT2 and SIRT7 expression was noted during progression from preneoplasia to squamous cell carcinoma.

The distinct pattern of SIRT1 expression, from negative to feeble in normal cervical mucosa to a very high expression in SIL and heterogeneous expression pattern in the neoplasia, is indicative of a differential role in the multistage cancer. The Ki67 labeling index is a measure of proliferation status, and its expression was only observed in the basal layer in SIL cases thereby indicating that cell division was restricted to basal epithelium. A direct association between proliferation as

**Fig. 2** Sirtuin expression and localization pattern in cervical cancer cells and keratinocyte. **a** Real-time PCR analysis for expression of SIRT1, SIRT2, and SIRT7 in cervical cancer cell lines (HeLa, SiHa) and immortalized keratinocyte counterpart cell line, HaCaT. The bar diagram shows the fold increase in sirtuin expression. Each real-time PCR reaction was performed in triplicate, and for sirtuin mRNA expression, all values were normalized against GAPDH mRNA levels. Data is represented as mean±SD fold change relative to control from three independent experiments. **b** Representative immunoblots showing expression of sirtuin isoforms in various cell lines. Tubulin served as a loading control. **c** A bar diagram showing fold change in sirtuin expression as evaluated for cervical cancer cells (SiHa and HeLa) in relation to the immortalized cell counterpart, HaCaT. Each bar represents mean±SD of replicate experiments (\* $P < 0.05$ ). **d** Representative immunofluorescence images showing localization pattern of sirtuin members (*green*) in SiHa and HaCaT cells. SIRT1 showed prominent localization in the nucleus, SIRT2 was localized to the cytoplasm, and a prominent nucleolar localization of SIRT7 was noted. Cells were counterstained with DAPI (*blue*)

measured by Ki67 index and SIRT1 levels could not be ascertained in the preneoplastic intraepithelial lesions. In fact, the Ki67-negative non-dividing and differentiated cells in the top 1st/3rd portion of epithelium were also strongly positive for SIRT1 expression. On the other hand, a significant statistical association was found between SIRT1 and p27 expression in the squamous intraepithelial lesions. Although we did not find any difference in SIRT1 expression among the low SIL and high SIL grades. Overall, the uniform higher expression levels are indicative of SIRT1 as a strong candidate marker for preneoplasia. Unlike the preneoplasia, the SIRT1 expression showed a heterogeneous staining pattern in squamous cell carcinoma. Our results are quite similar to those of an earlier report, where SIRT1 levels are high in benign adenomas of the colon and varied in SCC ranging from high to low [39]. We propose three different scenarios for the intriguing pattern of SIRT1 expression during progression from preneoplasia to SCC. Firstly, a strong association between SIRT1 and the growth arrest marker p27 in preneoplasia and its downregulation in a subset of SCC strongly point to its primary role in tumor suppression. However, a subset of tumors showed strong positivity for SIRT1; this in turn may be associated as a counteractive feedback effect for growth suppression, and this second possibility has to be further explored. SIRT1 deacetylates substrates especially the tumor-suppressor proteins such as p53, Rb, and WRN which in turn are involved in mediating growth arrest and DNA repair. Thus, it is argued that an increase in expression level of nuclear SIRT1 in a subset of SCC cases is actually a feedback mechanism to limit the proliferation of the transformed cells. A possible third scenario is that SIRT1 acquires a different function during neoplastic progression such that increased expression levels of SIRT1 in some cancers may contribute to cancer development and maintenance. In fact, an increase in cytoplasmic SIRT1 is noted in many transformed cells and tumor tissues [40]. In general, SIRT1 has been reported to





be overexpressed in mouse and human prostate cancer [16], breast cancer [41], and lymphomas [42].

In the present study, in contrast to the unusual expression pattern of SIRT1 in preneoplasia, both SIRT2 and SIRT7 were found to be overexpressed in the carcinoma compared to normal and preneoplastic lesions. A strong statistical association between nuclear expression of SIRT1 and SIRT2 that emerged in premalignant intraepithelial lesions is indicative of a possible crosstalk between the different sirtuins during the progressive intermediate stage for progression towards transformation. Previous reports in animals have indicated SIRT2 as a tumor suppressor, and on the contrary, higher levels of SIRT2 were noted in prostate cancer [43], hepatocellular carcinoma [44], and estrogen receptor-negative tumors [20].

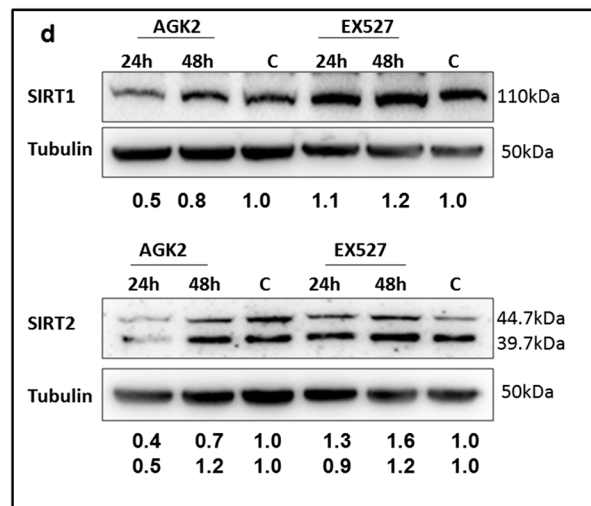
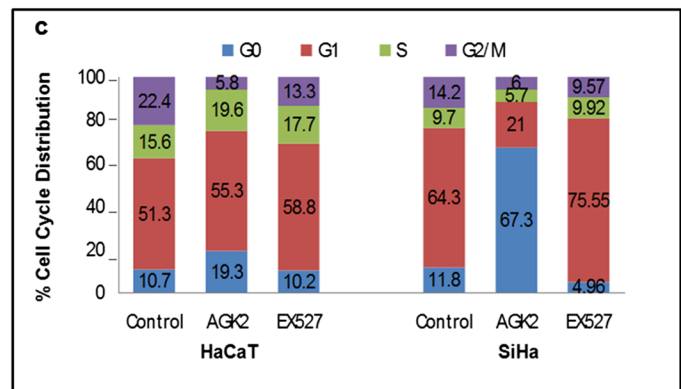
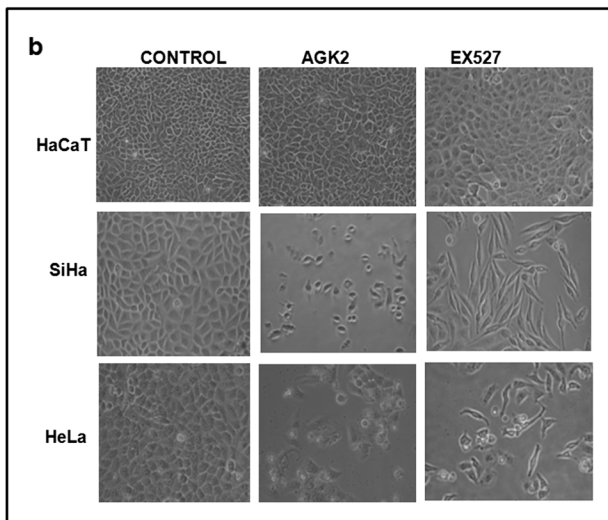
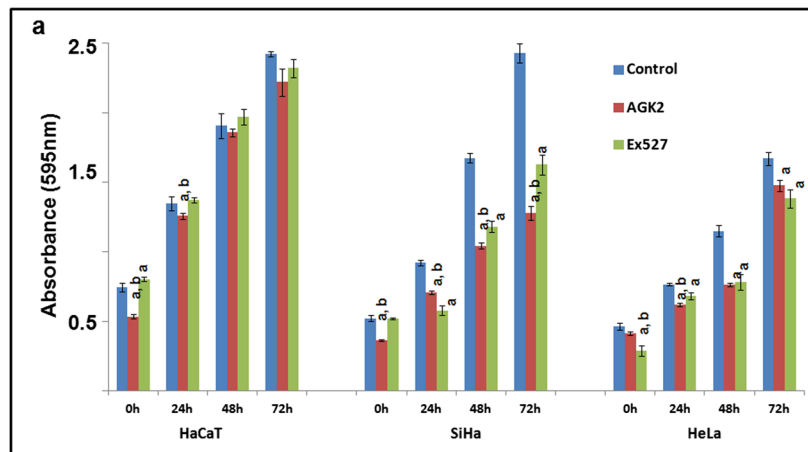
SIRT7 is the least studied sirtuin isoform. A recent study noted a higher expression of SIRT7 in hepatocellular carcinoma [17]. In the present study too, we found a good association between expression of cytoplasmic SIRT7 and cancer progression. SIRT7 is a known nuclear protein, and recently, we showed the existence of cytoplasmic SIRT7 in cell lines and also normal colonic epithelium [33]. By deacetylating the lysine 18 of histone 3 (H3K18), SIRT7 is known to play a role in maintenance of neoplastic transformed state [13]. The progressive increase in SIRT7 as seen in present study is indicative of its role in neoplastic continuance. Few studies have carried out a detailed analysis of all the sirtuin isoforms in any one particular cancer type. A study by Lai et al. [25] showed a downregulation of all the seven sirtuin isoforms in head and neck squamous cell cancer. While the study by McGlynn et al. [20] in breast cancer tumors revealed that, based on the tumor grade, SIRT2 can act as either a tumor suppressor or promoter. In our study too, the role of SIRT1 appears to depend on cellular context or tumor pathology.

Besides the primary tumors, we also studied the the expression and localization pattern of sirtuins in cervical cancer cell lines (HeLa and SiHa). The localization pattern of the three sirtuin members SIRT1, SIRT2, and SIRT7 appeared the same between the cancerous cell line and the immortalized near-normal cell counterpart (HaCaT). However, there appeared a difference in the levels of expression between the tumorigenic (HeLa and SiHa) and non-tumorigenic cell lines (HaCaT). The SIRT1 transcript and protein expression were significantly higher in the cancer cell lines compared to the non-tumorigenic counterpart. The SIRT2 mRNA expression did not show a significant increase; in contrast, a marked increase in protein level was observed in the tumorigenic cell lines. The increase in SIRT1 and SIRT2 protein expression in primary tissue was corroborated by the findings in the cervical cancer cell lines. However, unlike the

**Fig. 3** Effect of sirtuin inhibitors AGK2 (SIRT2) and Ex527 (SIRT1) on growth of cervical cancer cells. **a** Cellular survivability of cervical cancer cells (HeLa and SiHa) as measured by crystal violet dye uptake. Cells were treated with 20  $\mu$ M dose of AGK2 and Ex527 for 24 h and then released in fresh media followed by staining with crystal violet dye which were then extracted and the absorbance measured at 595 nm; cells treated with solvent alone (DMSO) served as a control. Note the growth inhibition in cervical cancer cells SiHa and HeLa following the treatment with sirtuin inhibitors. Letters *a* and *b* indicate significant difference with control and treatment with Ex527, respectively ( $P < 0.05$ ). **b** Phase-contrast images of cells treated with the sirtuin inhibitors. Note a change in morphology of both SiHa and HeLa cells when treated with Ex527. Note fewer cells following treatment with sirtuin inhibitors indicative of growth arrest. **c** A bar diagram showing the percent distribution of cells in various phases of cell cycle following treatment of cells with sirtuin inhibitor. Cells were fixed in ethanol, followed by propidium iodide staining, and ploidy status was checked by flow cytometry. Note in SiHa cells a prominence of sub G0 cells indicative of cell death when treated with AGK2, while an increase in G0/G1 cell population when treated with EX527, indicative of growth arrest. No significant changes were observed in HaCaT cells treated with the sirtuin inhibitors. **d** SIRT1 and SIRT2 protein expression following treatment of cells with their specific inhibitors EX527 and AGK2, respectively. HeLa cells were treated with 20  $\mu$ M for 24 h following which either the cell homogenate was made immediately (24 h) or medium was replaced with fresh medium and homogenate was prepared the next day (48 h). Cells treated with DMSO alone served as control (C) group. Tubulin served as a loading control. Values below the blot indicate the fold change in sirtuin levels following treatment with inhibitors relative to untreated control

squamous cell carcinomas which showed higher SIRT7 levels, the cervical cancer cell lines showed comparable expression to non-tumorigenic cells, and presently, it is not clear why these differences exist for SIRT7. Nonetheless, results of in vitro studies are indicative of both transcriptional and translational dependent mechanisms for SIRT1 overexpression in cancer cells. On the other hand, SIRT2 increase in cancer cells appear to be under a translational control, and further studies are needed in this regard.

In view of the overexpression of sirtuin isoforms in the cervical neoplasia, we evaluated the therapeutic potential of the sirtuin inhibitors. For this, the efficacy of the general sirtuin inhibitor, Sirtinol, and also the specific inhibitors of SIRT1 and SIRT2 were tested on growth and survival of cervical cancer cell lines. Interestingly, both Sirtinol and the SIRT2 inhibitor, AGK2, induced cell death, suggesting that these inhibitors may find application in treatment of cervical malignancy. In contrast, the SIRT1 inhibitor caused cytostasis due to cell cycle arrest. This indicates a differential mode of action of different sirtuin inhibitors. The growth inhibition via SIRT1 without leading to cell death is suggestive of its role in cell cycle regulation. In fact, inhibition of SIRT1 has been earlier proposed for a variety of cancer treatments [29]. Mostly, the sirtuin inhibitors affect the catalytic activity and hence the functioning of sirtuins; however, it was



noted in the present study that AGK2 which is a specific SIRT2 inhibitor also has a subtle influence on the stability of both SIRT1 and SIRT2 proteins at least in the initial

time points following treatment. This unusual finding warrants further studies and also questions its isoform specificity.

## Conclusion

The present study has shown the modulation of sirtuin levels in pathogenesis of cervical cancer. A progressive increase in levels of SIRT2 and SIRT7 was noted during cervical cancer progression. However, the specific increase in SIRT1 only in the benign lesion makes it a probable candidate in identification of intraepithelial precancerous lesions of the cervix. Further, inhibiting sirtuins appear as a promising therapeutic drug target in cervical cancer.

**Acknowledgments** We thank Dr. Lucy M. Anderson for the valuable suggestions, critical reading, and editing. SS is supported by a fellowship from the Department of Biotechnology. Laboratory of GR is supported by the funding from the Department of Biotechnology, New Delhi, India. We thank Mr. Bala for the help in flow cytometry. We thank Dr Nirupama Chatterjee for the help with statistical analysis. The critical comments and suggestions from the anonymous reviewers have helped immensely to improve the manuscript.

**Conflicts of interest** None

**Author contribution** SS performed all the experiments with the help from ST and SK. PAR helped in immunohistochemistry; BS and SS helped in immunoblotting. VVR performed the statistical analysis. The pathological evaluations were by UK. GR designed the study and wrote the manuscript with inputs from SS.

## References

- Haigis MC, Sinclair DA. Mammalian sirtuins: biological insights and disease relevance annual review of pathology: mechanisms of disease. *Annu Rev Pathol Mech Dis*. 2010;5:253–95.
- Nogueiras R, Habegger KM, Chaudhary N, Finan B, Banks AS, Dietrich MO, et al. Sirtuin 1 and sirtuin 3: physiological modulators of metabolism. *Physiol Rev*. 2012;92:1479–14.
- Polito L, Kehoe PG, Forloni G, Albani D. The molecular genetics of sirtuins: association with human longevity and age-related diseases. *Int J Mol Epidemiol Genet*. 2010;1:214–25.
- Presegue LB, Vaquero A. Dual role of sirtuins in cancer. *Gene Cancer*. 2011;2:648–62.
- Deng CX. SIRT1, is it a tumor promoter or tumor suppressor? *Int J Biol Sci*. 2009;5:147–52.
- Vaziri H, Dessain SK, Ng Eaton E, Imai SI, Frye RA, Pandita TK, et al. hSIR2 (SIRT1) functions as an NAD-dependent p53 deacetylase. *Cell*. 2001;107:149–59.
- Li S, Banck M, Mujtaba S, Zhou MM, Sugrue MM, Walsh MJ. p53-induced growth arrest is regulated by the mitochondrial SirT3 deacetylase. *PLoS One*. 2010;5:e10486.
- Wang R, Sengupta K, Li C, Kim H, Cao L, Xiao C, et al. Impaired DNA damage response, genome instability, and tumorigenesis in SIRT1 mutant mice. *Cancer Cell*. 2008;14:312–23.
- Kim HS, Patel K, Jacobs KM, Bisht KS, Aykin-Burns N, Pennington JD, et al. SIRT3 is a mitochondrial-localized tumor suppressor required for maintenance of mitochondrial integrity and metabolism during stress. *Cancer Cell*. 2010;17:41–52.
- North BJ, Verdin E. Mitotic regulation of SIRT2 by cyclin-dependent kinase 1-dependent phosphorylation. *J Biol Chem*. 2007;282:19546–55.
- Jeong SM, Xiao C, Finley LWS, Lahusen T, Souza AL, Pierce K, et al. SIRT4 has tumor-suppressive activity and regulates the cellular metabolic response to DNA damage by inhibiting mitochondrial glutamine metabolism. *Cancer Cell*. 2013;23:450–63.
- Van Meter M, Mao Z, Gorbunova V, Seluanov A. Repairing split ends: SIRT6, mono-ADP ribosylation and DNA repair. *Aging*. 2011;3:829–35.
- Barber MF, Michishita-Kioi E, Xi Y, Tasselli L, Kioi M, Mogtaderi Z, et al. SIRT7 link H3K18 deacetylation to maintenance of oncogenic transformation. *Nature*. 2012;487:114–8.
- Cha EJ, Noh SJ, Kwon KS, Kim CY, Park BH, Park HS, et al. Expression of DBC1 and SIRT1 is associated with poor prognosis of gastric carcinoma. *Clin Cancer Res*. 2009;15:4453–9.
- Ahuja N, Li Q, Mohan AL, Baylin SB, Issa JP. Aging and DNA methylation in colorectal mucosa and cancer. *Cancer Res*. 1998;58:5489–94.
- Huffman DM, Grizzle WE, Bamman MM, Kim JS, Eltoum IA, Elgavish A, et al. SIRT1 is significantly elevated in mouse and human prostate cancer. *Cancer Res*. 2007;67:6612–8.
- Chen J, Zhang B, Wong N, Lo AWI, To KF, Chang AWH, et al. Sirtuin 1 is upregulated in a subset of hepatocellular carcinomas where it is essential for telomere maintenance and tumor cell growth. *Cancer Res*. 2011;71:4138–49.
- Kim JK, Noh JH, Jung KH, Eun JW, Bae HJ, Kim MG, et al. Sirtuin7 oncogenic potential in human hepatocellular carcinoma and its regulation by the tumor suppressors MiR-125a-5p and MiR-125b. *Hepatology*. 2013;57:1055–67.
- Kim HS, Vassilopoulos A, Wang RH, Lahusen T, Xiao T, Xu X, et al. SIRT2 maintain genomic integrity and suppresses tumorigenesis through regulating APC/C activity. *Cancer Cell*. 2011;20:487–99.
- McGlynn LM, Zino S, MacDonald AI, Curle J, Reilly JE, Mohammed ZM, et al. SIRT2: tumor suppressor or tumor promoter in operable breast cancer. *Eur J Cancer*. 2014;50:290–301.
- Finley LW, Carracedo A, Lee J, Souza A, Egia A, Zhang J, et al. SIRT3 opposes reprogramming of cancer cell metabolism through HIF1 $\alpha$  destabilization. *Cancer Cell*. 2011;19:416–28.
- Alhazzazi TY, Kamarajan P, Joo N, Huang JY, Verdin E, D'Silva NJ, et al. Sirtuin-3(SIRT3), a novel potential therapeutic target for oral cancer. *Cancer*. 2011;117:1670–8.
- Marquardt JU, Fischer K, Teufel A, Krupp M, Thorgeirsson SS, Galle PR, et al. Loss of SIRT6 in hepatocellular carcinoma: associated molecular traits and clinical implications. *Z Gastroenterol*. 2012;50:5–34.
- Benavente CA, Schnell SA, Jacobson EL. Effects of niacin restriction on sirtuin and PARP responses to photodamage in human skin. *PLoS One*. 2012;7:e42276.
- Lai CC, Lin PM, Lin SF, Hsu CH, Lin HC, Hu ML, et al. Altered expression of SIRT gene family in head and neck squamous cell carcinoma. *Tumor Biol*. 2013;34:1847–54.
- Allison SJ, Jiang M, Milner J. Oncogenic viral protein HPV E7 up-regulates the SIRT1 longevity protein in human cervical cancer cells. *Aging*. 2009;1:316–27.
- Michishita E, Park JY, Burneskis JM, Barrett JC, Horikawa I. Evolutionarily conserved and nonconserved cellular localizations and functions of human SIRT proteins. *Mol Biol Cell*. 2005;16:4623–35.
- Kiran S, Anwar T, Kiran M, Ramakrishna G. Sirtuin 7 in cell proliferation, stress and disease: rise of the seventh Sirtuin! *Cell Signal*. 2015;3:673–82.
- Villalba JM, Alc ain FJ. Sirtuin activators and inhibitors. *Biofactors*. 2012;38:349–59.
- Feng W, Xiao J, Zhang Z, Rosen DG, Brown RE, Liu J, et al. Senescence and apoptosis in carcinogenesis of cervical squamous carcinoma. *Mod Pathol*. 2007;20:961–6.
- Lomnytska MI, Becker S, Bodin I, Olsson A, Hellman K, Hellstr m A-C, et al. Differential expression of ANXA6, HSP27, PRDX2,

- NCF2, and TPM4 during uterine cervix carcinogenesis: diagnostic and prognostic value. *Br J Can.* 2011;104:110–9.
32. Ram BM, Ramakrishna G. Endoplasmic reticulum vacuolation and unfolded protein response leading to paraptosis like cell death in cyclosporine A treated cancer cervix cells is mediated by cyclophilin B inhibition. *Biochim Biophys Acta.* 2014;1843(11):2497–512.
  33. Kiran S, Chatterjee N, Singh S, Kaul SC, Wadhwa R, Ramakrishna G. Intracellular distribution of human SIRT7 and mapping of the nuclear/nucleolar localization signal. *FEBS J.* 2013;280:3451–66.
  34. Livak KJ, Schmittgen TD. Analysis of relative gene expression data using real-time quantitative PCR and the  $2^{-\Delta\Delta C(T)}$  Method. *Methods.* 2001;25:402–8.
  35. Maxwell MM, Tomkinson EM, Nobles J, Wizeman JW, Amore AM, Quinti L, et al. The Sirtuin 2 microtubule deacetylase is an abundant neuronal protein that accumulates in the aging CNS. *Hum Mol Genet.* 2011;15:3986–96.
  36. Chhabra S, Bhavani M, Mahajan N, Bawaskar R. Cervical cancer in Indian rural women: trends over two decades. *J Obstet Gynaecol.* 2010;30:725–8.
  37. Munoz N, Castellsague X, de Gonzalez AB, Gissmann L. Chapter 1: HPV in the etiology of human cancer. *Vaccine.* 2006;24(S3):1–10.
  38. Ota H, Tokunaga E, Chang K, Hikasa M, Iijima K, Eto M, et al. Sirt1 inhibitor, Sirtinol, induces senescence-like growth arrest with attenuated Ras-MAPK signaling in human cancer cells. *Oncogene.* 2006;25:176–85.
  39. Kabra N, Li Z, Chen L, Li B, Zhang X, Wang C, et al. Sirt1 is an inhibitor of proliferation and tumor formation in *colon cancer*. *J Biol Chem.* 2009;284:18210–7.
  40. Byles V, Chmielewski LK, Wang J, Zhu L, Forman LW, Faller DV, et al. Aberrant cytoplasm localization and protein stability of SIRT1 is regulated by PI3K/IGF-1R signalling in human cancer cells. *Int J Biol Sci.* 2010;6:599–612.
  41. Kuo SJ, Lin HY, Chien SY, Chen DR. SIRT1 suppresses breast cancer growth through downregulation of Bcl-2 protein. *Oncol Rep.* 2013;30:125–30.
  42. Jang KY, Hwang SH, Kwon KS, Kang MJ, Lee DG, Kim HS, et al. SIRT1 expression is associated with poor prognosis of diffuse large B-cell lymphoma. *Am J Surg Pathol.* 2008;32:1523–31.
  43. Hou H, Chen W, Zhao L, Zuo Q, Zhang G, Zhang X, et al. Cortactin is associated with tumor progression and poor prognosis in prostate cancer and SIRT2 other than HADC6 may work as facilitator in situ. *J Clin Pathol.* 2012;65:1088–96.
  44. Chen J, Chan AW, To KF, Chen W, Zhang Z, Ren J, et al. SIRT2 overexpression in hepatocellular carcinoma mediates epithelial to mesenchymal transition by protein kinase B/glycogen synthase kinase-3 $\beta$ / $\beta$ -catenin signaling. *Hepatology.* 2013;57:2287–98.